Rectification of Spatial Disorder

Jaegon Um,[1] Hyunsuk Hong,[2] Fabio Marchesoni,[3] and Hyunggyu Park[1]
[1]School of Physics, Korea Institute for Advanced Study, Seoul 130-722, Korea
[2]Department of Physics, Chonbuk National University, Jeonju 561-756, Korea
[3]Scuola di Scienze e Tecnologie, Università di Camerino, I-62032 Camerino, Italy
(Received 25 April 2011; published 7 February 2012)

We demonstrate that a large ensemble of noiseless globally coupled-pinned oscillators is capable of rectifying spatial disorder with spontaneous current activated through a dynamical phase transition mechanism, either of first or second order, depending on the profile of the pinning potential. In the presence of an external weak drive, the same collective mechanism can result in an absolute negative mobility, which, though not immediately related to symmetry breaking, is most prominent at the phase transition. Our results apply to a tug-of-war by competing molecular motors for bidirectional cargo transport.

DOI: 10.1103/PhysRevLett.108.060601 PACS numbers: 05.60.−k, 05.45.Xt, 64.60.−i

Rectifiers are special devices capable of extracting a steady output signal (current) even from a perfectly center-symmetric input signal (drive) [1]. Their minimal operating conditions typically require an asymmetric internal dynamics, possibly chosen to optimize performance, and a nonstationary unbiased input signal, mostly a cyclostationary periodic drive or a time-correlated noise. In thermodynamical terms, rectifiers are devices that operate under nonequilibrium conditions. Direction and magnitude of their output current strongly depend on both the drive(s) (intensity and time scales) and their intrinsic noise (temperature). Rectifiers are often called ratchets or else, to emphasize the role played by thermal fluctuations, Brownian motors [2].

To explore the possibility of replacing temporal variability by spatial randomness as a rectification source, we consider a system of N pinned phase oscillators coupled through the Kuramoto-type global interaction [3],

$$\dot{\phi}_i = \omega_i + f_e - V'(\phi_i) - (K/N)\sum_{j=1}^{N}\sin(\phi_i - \phi_j), \quad (1)$$

where ϕ_i and ω_i denote, respectively, the phase and the intrinsic frequency of the i-th oscillator. The intrinsic frequencies are assumed to be randomly distributed according to a Gaussian distribution function, $g(\omega)$, with zero mean and variance σ_ω; a tunable frequency bias is introduced by the external drive f_e. The third and fourth term on the right-hand side represent the pinning force acting on the ith oscillator and the all-to-all ferromagnetic ($K > 0$) coupling between oscillators, respectively. Because of the global nature of the interactions, mean-field- (MF-)type phase transitions are expected [4]. The on-site pinning potential $V(\phi)$ is taken to be the same for all oscillators as, with $V'(\phi) = dV/d\phi$,

$$V(\phi) = -a\cos\phi + (b/2)\cos 2\phi. \quad (2)$$

This model can serve as a stylized description of intracellular cargo transport by an array of interacting molecular motors walking along one or more polarized filaments [5–7]. The phase ϕ_i and the frequency ω_i can be interpreted as the position and the intrinsic velocity of the ith molecular motor. Its independent pulling or pushing force results in randomly distributed intrinsic velocities. A periodic bistable pinning potential would then mimic, for instance, the binding interaction of a two-headed molecular motor stepping along a spatially structured filament. In one period of motion, a molecular motor moves (by carrying or pushing a cargo) a distance of $\Delta\phi = 2\pi$ by executing two consecutive steps. Such steps are characterized by different lengths and activation energies, depending on the stoichiometry of two motor heads as well as on the chiral structure of the underlying filament. In addition, the sinusoidal Kuramoto coupling promotes a march in step between interacting motor pairs (phase synchronization) [3]. The same model can also be invoked to describe the operation of coupled artificial nanofabricated motors, where short carbon nanotubes can rotate and/or translate along fibers of inner nanotubes subjected to random thermal gradients [8].

Strong cooperative effects among molecular motors are ensured by assuming global pair coupling, irrespective of spatial separation. Such global coupling is known to well describe the attractive motor-motor interactions mediated by the underlying filaments [6]. Detachment of motors off the filaments is ignored in our model, as most biomolecular motors are, indeed, strongly processive. As the effects of the weak temporal fluctuations at the short, or transient, time scales of practical interest are negligible, we focus here on the noiseless dynamics of our model.

Despite ignoring the specific details of the molecular motor structure and operation (including low-dimensional short-range interactions or more complicated coupling potentials), this model has the practical advantage that it

can be treated analytically in a MF scheme. MF approaches are often used to gain a first qualitative understanding of many-body effects. The present case is no exception: our MF analysis reveals that the bi- (or multi-)stability of the pinning potential, combined with the global ferromagnetic motor pair coupling, is responsible for a collective march-in-step of the entire motor ensemble.

The onset of spontaneous currents has already been reported for this system in the regime of $N \to \infty$ and finite temperatures [1,4]. For zero drive, $f_e = 0$, the dynamics of Eq. (1) has no built-in spatial asymmetry; thus, a nonzero current can only occur as a collective or many-body effect, i.e., by spontaneous symmetry breaking (SSB). Adding an external load, $f_e \neq 0$, breaks the symmetry, thus causing a driven current. However, under certain conditions, such current may happen to be oriented against the load, a counterintuitive nonlinear phenomenon called absolute negative mobility (ANM) [4,9]. Both effects have been studied under conditions where thermal noise plays a prominent role and, therefore, have been interpreted as noise induced rectification phenomena [4,10]. In fact, temporal fluctuations, no matter how weak, affect the SSB mechanism itself. For instance, at zero drive and finite temperatures, the reported spontaneous currents have been explained as a manifestation of dynamic phase transitions of the second order [4].

In this Letter, we consider a large ensemble of Kuramoto oscillators in a quenched disordered landscape at zero temperature. Contrary to the earlier literature, here spontaneous currents can solely result from the rectification of the spatial disorder. Most remarkably, the dynamic phase transitions responsible for their activation, can be either of first or second order, depending on the degree of bistability of the pinning potential. Indeed, such dynamic phase transitions follow directly the SSB of the discrete Ising symmetry of $V(\phi)$. Moreover, we observe that ANM is neither induced by thermal noise, nor immediately related to symmetry breaking, although its magnitude is most prominent at the phase transition.

As the coordinates ϕ_i are not coupled to a heat bath, the ergodic assumption does not apply here, that is, the oscillator dynamics can depend on the initial conditions (IC), $\{\phi_i(0)\}$. The simulation data reported below refer to the case of disordered IC, where $\{\phi_i(0)\}$ have been uniformly randomized in the interval $(0, 2\pi)$. We also simulated ordered initial configurations with pinned phases and even annealing procedures. We found that the key conclusions of our MF analysis do not change.

The local dynamics of Eq. (1) is controlled by the on-site pinning potential of Eq. (2): it is symmetric, $V(-\phi) = V(\phi)$, and periodic in ϕ with period 2π. Its unit cells are monostable with one minimum at $\phi = 0 \pmod{2\pi}$ for $b \leq a/2$, and bistable with two stable points at $\phi = \pm\phi_m$ for $b > a/2$, where $\phi_m = \arccos(a/2b)$. Isolated oscillators are symmetrically locked for $|\omega_i + f_e| < f_p$ with locking phases $|\phi_i| < \phi_p$, where the largest locking phase ϕ_p is the (larger) positive solution of the equation $V''(\phi) = 0$ and the depinning frequency threshold is $f_p = V'(\phi_p)$.

The nontrivial global dynamics of the system is controlled by the oscillator coupling constant K. Following Kuramoto's approach [3], we introduce the synchronization order parameter Δ and the average phase θ, defined by $\Delta e^{i\theta} \equiv \langle e^{i\phi_j} \rangle$, where $\langle O_j \rangle = (1/N)\sum_{j=1}^{N} O_j$ denotes the oscillator ensemble average. Accordingly, Eq. (1) can be rewritten as

$$\dot{\phi}_i = \omega_i + f_e - U'(\phi_i), \tag{3}$$

with the effective potential $U(\phi)$ given by

$$U(\phi) = V(\phi) - K\Delta\cos(\phi - \theta). \tag{4}$$

Here, the parameters Δ and θ are determined through the self-consistency relations

$$C = \Delta\cos\theta = \langle\cos\phi_j\rangle, \qquad S = \Delta\sin\theta = \langle\sin\phi_j\rangle. \tag{5}$$

For $\theta = 0$, the potential $U(\phi)$ is characterized by the depinning frequency thresholds $\pm\tilde{f}_p$, the corresponding depinning phases $\pm\tilde{\phi}_p$, and, if bistable, the two symmetric minima at $\phi = \pm\tilde{\phi}_m$, similar to the isolated oscillators. The interaction term in $U(\phi)$ tends to suppress the bistability of the pinning potential even for $b > a/2$: $U(\phi)$ is bistable only for small K, $0 \leq K < K_w$, where the bistability threshold K_w is the solution of the implicit equation of $K_w\Delta(K_w) = 2b - a$. For $\theta \neq 0$, $U(\phi)$ is no longer mirror symmetric; correspondingly, the symmetric depinning thresholds, $\pm\tilde{f}_p$, are replaced by two distinct thresholds, $\tilde{f}_p^{\pm}(K, f_e)$, with $\tilde{f}_p^{+} \neq -\tilde{f}_p^{-}$.

For $f_e = 0$, the antisymmetry of Eq. (3) guarantees $\phi(\omega) = -\phi(-\omega)$ as long as $\theta = 0$, so that the current $J = \langle\dot{\phi}\rangle/2\pi$ is identically zero. A net SSB current sets on only for $\theta \neq 0$, where two distinct frequency thresholds ($\tilde{f}_p^{+} \neq -\tilde{f}_p^{-}$) break the left-right symmetry of the running oscillators. As the pinning ensures a certain degree of synchronization ($\Delta > 0$ at all $K \geq 0$), the average phase θ alone (or more conveniently S) becomes the proper order parameter of the system. Supersymmetry considerations [1] rule out spontaneous currents for a purely harmonic pinning potential ($a = 0$ or $b = 0$). A biharmonic $V(\phi)$, instead, allows nonzero S and J in the strong coupling regime of $K > K_c$. The transition threshold K_c is actually a function of two parameters only, σ_ω and b, since a can be rescaled to unity without loss of generality.

To investigate a large ensemble of disordered oscillators, we had recourse to the numerical integration of the equations of motion, Eq. (1), for the entire ensemble. For the sake of a comparison, we also numerically solved the self-consistency equations, Eqs. (3)–(5) [11]. In Fig. 1, we compare the dependence of K_c and K_w on the pinning bistability parameter b at $f_e = 0$. The intersection of $K_c(b)$ and $K_w(b)$ at $b = b^*$ defines two distinct dynamical

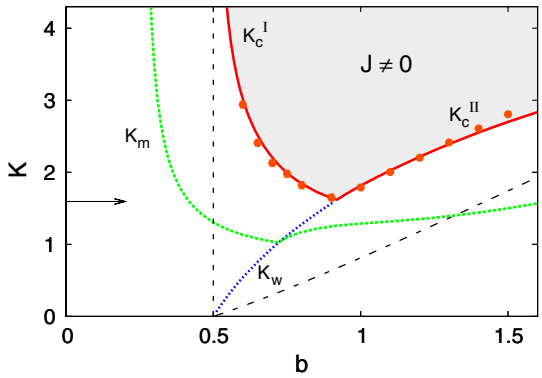

FIG. 1 (color online). Phase diagram at $f_e = 0$. The thresholds of SSB (K_c), global bistability (K_w), and ANM (K_m), are plotted versus b when $\sigma_\omega = a = 1$. All curves are obtained by analyzing Eqs. (3)–(5) in the mean-field approximation. Numerical data (dots) are obtained by integrating Eq. (1) with $N = 10^6$, starting from random initial conditions. The two transition branches (K_c^I and K_c^{II}) are connected by a cusp at $(K^*, b^*) \simeq (1.68, 0.94)$. The dashed curves are the analytic limits of K_c^I and K_c^{II} for $\sigma_\omega = 0$, i.e., $g(\omega) = \delta(\omega)$; the horizontal arrow indicates the critical coupling for the unpinned Kuramoto model, $\sqrt{8/\pi}\sigma_\omega$.

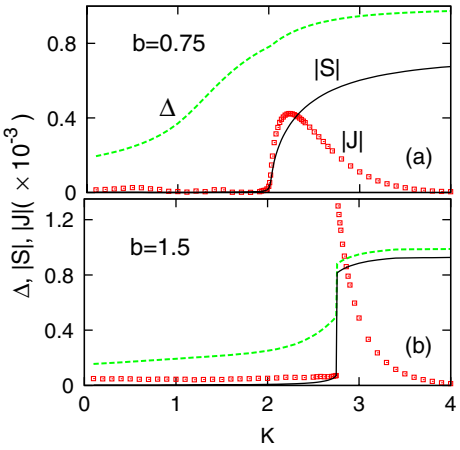

FIG. 2 (color online). Spontaneous currents. $|J|$ (squares), Δ (dashed) and $|S|$ (solid) versus K (a) in region I at $b = 0.75$, and (b) in region II at $b = 1.5$, from the numerical integration of Eq. (1).

regimes: (i) region I ($a/2 < b < b^*$). The SSB transition occurs after the pinning bistability is completely suppressed by the Kuramoto coupling ($K_c^I > K_w$). The transition branch K_c^I diverges as $b \to a/2$ as expected and decays toward a minimum at $b = b^*$; (ii) region II ($b > b^*$). The transition branch K_c^{II} always lies below K_w [12], so SSB occurs inside the bistability regime where multiple solutions are possible. Moreover, we notice that $K_c^I(b)$ and $K_c^{II}(b)$ form a cusp at $b = b^*$, which indicates that two different SSB mechanisms are at work in regions I and II.

Following this lead, we numerically computed the spontaneous current, J, as a function of K at $b = 0.75$ in region I and $b = 1.5$ in region II, see Fig. 2. The difference is revealing: The onset of J can be regarded as a dynamical phase transition of the second order, with

$$|J| \propto (K - K_c)^{1/2}, \tag{6}$$

in region I, and of the first order, in region II. In the latter, $|J|$ jumps discontinuously from 0 to a maximum at $K = K_c^{II}$, and finally decays exponentially at larger K. Similar continuous or discontinuous behaviors at the transition points are exhibited by the corresponding order parameters Δ and S. No first-order transitions were detected in the presence of thermal noise [4].

The existence of a nonzero SSB current for $K > K_c^I$ can be analytically explained in region I by linearizing Eqs. (3)–(5) for small $S \simeq \Delta\theta$. A net current can only result from the oscillators running, respectively, to the right with $\omega > \tilde{f}_p^+$ and to the left with $\omega < \tilde{f}_p^-$. In the linear regime, it is easy to find from Eqs. (3) and (4) $\tilde{f}_p^\pm \simeq \pm\tilde{f}_p + K|\cos\tilde{\phi}_p|S$, which yields the net current J for small drive f_e

$$2\pi J \propto -(\tilde{f}_p^+ + \tilde{f}_p^-)/2 \simeq f_e - K|\cos\tilde{\phi}_p|S. \tag{7}$$

Here, Eq. (7) implies a linear response also to the external drive f_e, which will be discussed later. At $f_e = 0$, $J \propto -S$ near the transition.

The critical behavior of S near the transition can be also extracted by linearizing the self-consistency Eqs. (5) at $f_e = 0$. Since the system has the Ising-like Z_2 symmetry, the second self-consistency relation for S can be expanded in odd powers as

$$S = (K/K_c)S - \kappa S^3 + \mathcal{O}(S^5). \tag{8}$$

With $\kappa > 0$, we find the stable solution of $S = 0$ for $K \leq K_c^I = K_c$ and a new stable branch of $S \propto (K - K_c^I)^{1/2}$ for $K \gtrsim K_c^I$, which determines the MF critical exponent of the current in Eq. (6).

The first-order transition along $K_c^{II}(b)$ in region II is a unique feature of our model. It occurs where the static phase solution of Eq. (3) for the locked oscillators consists of two disconnected branches, $\phi_{1,2}(\omega)$, with $\phi_1(-\omega) = -\phi_2(\omega)$ in a small ω interval centered around $\omega = 0$. For a homogeneous randomization of the initial phases, both solutions $\phi_{1,2}(\omega)$ contribute to the ensemble averages with statistical weights proportional to the respective basin size. For oscillators with $\omega = 0$, these weights are equal at $\theta = 0$. As θ departs from zero, the symmetry of two branches is broken, but the deterministic nature of dynamics does not allow the system to redistribute the oscillator ensemble across the gap separating two solutions (as it would in the presence of noise [4]). Such a resistance of the system against perturbations reflects itself in a delayed onset of the SSB phase in region II; as a consequence, κ becomes negative well before the transition, which causes

a discontinuous jump in θ at the transition. Indeed, the SSB transition is delayed until the $S = 0$ solution becomes locally unstable. Therefore, the transition threshold K_c^{II} is again determined by the linear term in Eq. (8), with the difference that for $\kappa < 0$ (at the transition) the stable solution of S exhibits a discontinuity.

The reentrant profile of the transition curve $K_c(b)$ can be explained qualitatively as follows: For a phase transition to occur, the average attractive Kuramoto force must win over disorder; i.e., $(K/2)\sin 2\phi_m$ must be larger than σ_ω. The nonmonotonicity of $\sin 2\phi_m$ in the range $0 \le \phi_m \le \pi/2$ determines the convexity of $K_c(b)$. In particular, $K_c(b)$ diverges in correspondence with the zeros of $\sin 2\phi_m$, like $\frac{1}{2}(b - a/2)^{-1/2}$ for $b \to a/2$, and proportional to $2b$ for $b \to \infty$, in agreement with Fig. 1. One may obtain a simpler but less accurate expression for K_c from the self-consistency equations as $1/K_c \simeq \langle \cos^2\phi / U''(\phi) \rangle$ [13], which becomes exact at $\sigma_\omega = 0$ for identical oscillators [14]. Its solutions exhibit, besides the two diverging branches for $b \to \infty$ and $b \to a/2$, also a suggestive lower bound at $b = b^*$ as $\sigma_\omega \sqrt{8/\pi}$, which happens to coincide with the critical coupling of the unpinned Kuramoto model [$V(\phi) \equiv 0$].

Further evidence of the coexisting phase transitions of the first and second order was obtained by investigating the system response to a finite bias f_e, and more specifically, by analyzing the driven current $J(f_e)$ and its zero-point mobility, $\mu_0 = (dJ/df_e)_{f_e=0}$. We computed both quantities by direct integration of Eq. (1) and summarized our results in Fig. 3. In panel (a), the characteristic curve J-f_e clearly exhibits three different regimes: (i) $0 < K < K_m$. Below a certain threshold K_m (also plotted versus b in Fig. 1), J is parallel to f_e as expected in the linear response theory ($\mu_0 > 0$); (ii) $K_m < K < K_c$. The drive modifies the global interaction of the oscillators with their pinning potential in such a fashion that the ensemble response points against the drive. The curve $J(f_e)$ is continuous at $f_e = 0$ with $\mu_0 < 0$ (ANM), and turns positive for larger f_e; (iii) $K > K_c$. The slope of $J(f_e)$ at the origin, μ_0, can grow so negative that eventually the curve splits into two disconnected antisymmetric branches with $J(0^+) = -J(0^-) < 0$ and uniquely defined negative μ_0 (ANM). This discontinuity is a signature of SSB and is a common feature of both regions I and II. Note that ANM occurs regardless of the presence of thermal noise.

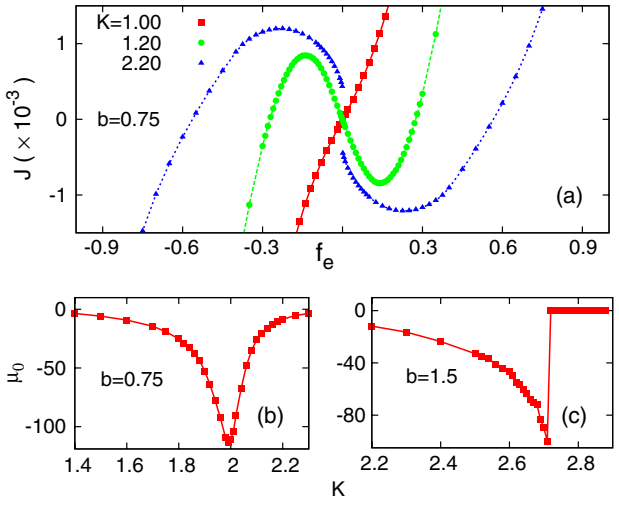

FIG. 3 (color online). Absolute negative mobility. (a) J-f_e characteristic curve for $b = 0.75$ and three different K from numerical integration of Eq. (1). (b),(c) μ_0 versus K in the vicinity of the transition point for (b) $b = 0.75$, and (c) $b = 1.5$. For graphical convenience, μ_0 has been rescaled by the factor $2\pi/\langle|\dot{\phi}|\rangle$.

The different SSB mechanisms of regions I and II also influence the ANM properties of the system, see Figs. 3(b) and 3(c). In region I, $\mu_0(K)$ develops an asymmetric negative peak numerically compatible with a two-sided divergence for $K \to K_c^{I\pm}$. In region II, $\mu_0(K)$ is clearly discontinuous with a negative diverging branch for $K \to K_c^{II-}$, and a slowly decaying one for $K > K_c^{II}$. In both regions, for exceedingly large or small coupling constants $\mu_0(K)$ tends to vanish, as expected. Finally, we remark that ANM does not necessarily anticipate SSB, as apparent in Fig. 1, where the curve $K_m(b)$ (marking the ANM onset) crosses into a region of the monostable pinning for $b < a/2$, inaccessible to $K_c(b)$.

The numerical results of Fig. 3 can be qualitatively understood from the linear response Eq. (7) for the current, which yields

$$\mu_0 \propto 1 - K|\cos\tilde{\phi}_p|\chi, \tag{9}$$

where $\chi = (dS/df_e)_{f_e=0}$ is the zero-field susceptibility. The curve $K_m(b)$ plotted in Fig. 1 was obtained, indeed, from Eq. (9) and then checked against the numerical integration data from Eq. (1). Note that $K_m(b)$ also develops a minimum (actually a cusp) as it crosses $K_w(b)$. Like in the ordinary equilibrium MF theory, one can find $\chi \propto |K_c - K|^{-\gamma}$ ($\gamma = 1$) near $K = K_c^I$ and, notably, also for $K \lesssim K_c^{II}$, where the local instability occurs around $S = 0$. Therefore, ANM also diverges at SSB transition point with MF susceptibility exponent $\gamma = 1$, which is consistent with our numerical results.

Our results can be easily generalized to models involving local pinning potentials with higher symmetry, for which we expect qualitatively similar features, such as continuous and first-order dynamic phase transitions, reentrant behavior, and ANM. The present analysis was based on a MF approximation, valid only when the motor-motor interaction is sufficiently long-ranged. An exhaustive description of the long-time dynamics of processive motors or, more in general, of spatially extended systems with short-range interactions, would additionally require an appropriate modeling of the fluctuating detachment-attachment dynamics.

H. P. thanks Changbong Hyeon for useful discussions and KIAS center for Advanced Computation for providing computing resources. This work was supported by the Basic Science Research Program of MEST, NRF grant No. 2011-0009697, and by the European Community, Grant No. 256959 (NanoPower).

[1] P. Reimann, Phys. Rep. **361**, 57 (2002).
[2] P. Hänggi and F. Marchesoni, Rev. Mod. Phys. **81**, 387 (2009).
[3] Y. Kuramoto, *Chemical Oscillations, Waves and Turbulence* (Springer, Berlin, 1984); J. A. Acebrón *et al.*, Rev. Mod. Phys. **77**, 137 (2005).
[4] J. Buceta, J. M. Parrondo, C. Van den Broeck, and F. J. de la Rubia, Phys. Rev. E **61**, 6287 (2000).
[5] F. Jülicher and J. Prost, Phys. Rev. Lett. **75**, 2618 (1995).
[6] M. Müller, S. Klumpp, and R. Lipowski, Proc. Natl. Acad. Sci. U.S.A. **105**, 4609 (2008); D. Hexner and Y. Kafri, Phys. Biol. **6**, 036016 (2009).
[7] V. Epshtein and E. Nudler, Science **300**, 801 (2003).
[8] A. Barreiro *et al.*, Science **320**, 775 (2008).
[9] R. Eichhorn, P. Reimann, and P. Hänggi, Phys. Rev. Lett. **88**, 190601 (2002); L. Machura, M. Kostur, P. Talkner, J. Luczka, and P. Hänggi, Phys. Rev. Lett. **98**, 040601 (2007); D. Speer, R. Eichhorn, and P. Reimann, Europhys. Lett. **79**, 10005 (2007).
[10] S. E. Mangioni, R. R. Deza, and H. S. Wio, Phys. Rev. E **63**, 041115 (2001); M. Kostur, J. Luczka, and L. Schimansky-Geier, Phys. Rev. E **65**, 051115 (2002); M. A. Zaks, A. B. Neiman, S. Feistel, and L. Schimansky-Geier, Phys. Rev. E **68**, 066206 (2003).
[11] In the regime of weak disorder, $\sigma_\omega \ll |\tilde{f}_p^{\pm}|$, the ensemble averages in Eqs. (5) can be restricted to static (pinned) oscillators only with $\omega \in (\tilde{f}_p^-, \tilde{f}_p^+)$. In this approximation, we can locate K_c very accurately.
[12] In region II, K_w is no longer simply given by the equation $K_w\Delta = 2b - a$, which is valid only at $\theta = 0$.
[13] This approximation is good in regime I for any b and in regime II for $b \to b^*$ and $b \to \infty$.
[14] For $\sigma_w = 0$, both branches can be obtained analytically (Fig. 1): K_c^I becomes a vertical line at $b = a/2$ and $K_c^{II} = 2b + (a/4b)(a - \sqrt{a^2 + 32b^2})$.